WORLD CONFERENCE ON TIMBER ENGINEERING 2025
BRISBANE, AUSTRALIA
Advancing Timber for the Future Built Environment

DEVELOPMENT OF GIR SYSTEM WITH HIGH TOUGHNESS COUPLER

K.Nagai[1], Y.Mori[2], T.Kayukawa[3], K.Tanaka[4], R.Inoue[5], N.Sato[6], K.Harada[7]

ABSTRACT: A novel Glued-in Rod (GIR) joint system with enhanced toughness performance has been developed in our laboratory. This system is particularly significant as it substantially reduces both manufacturing time and cost compared to the previously developed GIR joint system. In this study, horizontal loading tests were conducted to evaluate the moment-resisting performance of the column base joint using the newly developed high toughness coupler. For almost all specimens, the high toughness coupler reached the target displacement before it fractured, confirming excellent deformation performance.

KEYWORDS: GIR, joint, toughness, coupler, mid-rise wooden building

1 INTRODUCTION

In recent years, mid- to high-rise timber buildings have emerged as a global trend in the pursuit of a decarbonized society. In order to realize these buildings, structural performance exceeding conventional technology for wooden houses is required.
Several Glued-in Rod (GIR) joint systems have been developed in our laboratory[1]. The GIR joint system exhibits higher strength and stiffness than conventional wooden joint systems. However, conventional GIR joint systems exhibit limitations in deformation capacity and toughness due to brittle failure. Thus, a novel GIR joint system incorporating a toughness-enhancing connector, referred to as the toughness connector, was developed in our laboratory. This toughness connector consists of a single rod with a smooth section for yielding and deformation, and threaded sections at both ends for adhesive bonding. Several moment resistance tests were conducted by our team on beam-column joints utilizing this GIR joint system with a toughness connector, yielding satisfactory performance. However, since this toughness connector is fabricated by cutting threaded sections at both ends of a single pipe, it is necessary to adjust the length of the threaded sections according to the depth of the column, requiring custom manufacturing. This process involves significant costs and time in the manufacturing phase.
To address these issues, a novel GIR joint system has been developed. It is composed of two commercially available fully threaded bolts and a coupler with enhanced toughness performance.
First, tensile and compression tests were conducted to evaluate the performance of this high toughness coupler. Second, horizontal loading tests were conducted to evaluate the moment-resisting performance of the column base joint using the high toughness coupler. Preliminary experiments showed that the shear connector was carrying the tensile force, which prevented the elongation of the coupler. For a high toughness coupler to perform to its full potential, the shear connector needs to have low tensile strength and be able to resist only shear forces. Therefore, several surface treatments were applied to the surface of the shear connector, and pull-out tests were conducted to compare the adhesive strength. Using the shear connector with the surface treatment determined by these tests, horizontal load tests were conducted again on the column base joints.

[1] Kota Nagai, Oita Univ., Oita, Japan, v2157432@oita-u.ac.jp

[2] Yuta Mori, Oita Univ., Oita, Japan, v2157445@oita-u.ac.jp

[3] Takato Kayukawa, Oita Univ., Oita, Japan, v24e5003@oita-u.ac.jp

[4] Kei Tanaka, Oita Univ., Oita, Japan, kei@oita-u.ac.jp

[5] Ryo Inoue, Kumamoto Univ., Kumamoto, Japan, rinoue@arch.kumamoto-u.ac.jp

[6] Naoto Sato, TOJU CORPORATION, Fukushima, Japan, tec6@toju.co.jp

[7] Koji Harada, WOOD STRUCTURE PROM INC., Tokyo, Japan, cozy_in_woodstock@nifty.com

https://doi.org/10.52202/080513-0374

2 TENSILE AND COMPRESSION TESTS OF HIGH TOUGHNESS COUPLER

2.1 SPECIMENS

Table 1 shows the list of specimens, Fig.1 shows the detail of the high toughness coupler, Fig.2 shows the specimen of the tensile test, and Fig.3 shows the specimen of the compression test.
The high toughness coupler was fabricated from steel pipe (JIS: STKM13A), and its length was designed with a target elongation of 20 mm at fracture. The outer diameter of the ductile section was controlled to ensure that the fracture load of the coupler was lower than the bond failure load of the fully threaded bolt. Additionally, internally threaded processing was applied to both ends of the coupler to accommodate the embedding of the fully threaded bolts.

Table 1 List of specimens

	Tree Species	Cross-Sectional Dimensions (mm)	Embedment Length (Anchorage Length) (mm)	Number of Specimens
Tensile Test	Sugi (E65-F225)	150×150	490 (378)	3
Compression Test	Sugi (E65-F225)	150×150	135	2

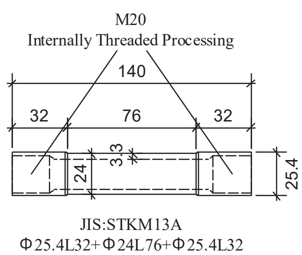

Fig.1 Details of the high toughness coupler

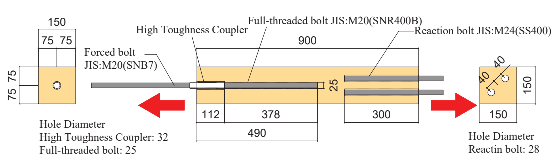

Fig.2 Specimen of the tensile test

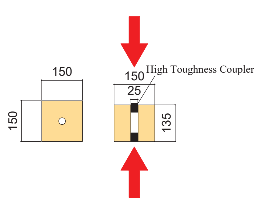

Fig.3 Specimen of the compression test

2.2 METHOD OF TENSILE AND COMPRESSION TEST OF HIGH TOUGHNESS COUPLER

A universal testing machine was used for loading in the tensile and compression tests, and monotonic tension and loading were applied at a speed of 1.0 mm/min.

2.3 RESULTS AND DISCUSSIONS

Fig.4 shows the relation between load and displacement of the typical specimens in tensile and compression tests. Table 2 shows characteristic properties obtained from tensile and compression tests.
In the tensile tests, the fracture displacement of all specimens was more than 20 mm. Comparing yield strength and ultimate strength in the tensile and compression tests, the values were almost equal, confirming that the tensile strength and compressive strength of this coupler are nearly equivalent. And, it was found to have the desired stiffness as well as deformation capability.

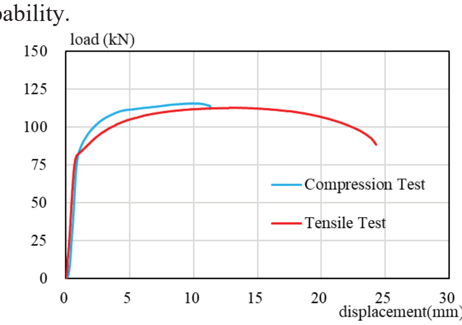

Fig.4 Relation between load and displacement

Table 2 Characteristic properties

	No.	Initial Stiffness (kN/mm)		Yield Strength (kN)		Ultimate Strength (kN)		Fracture Displacement (mm)		Plasticity Ratio	
		K	Ave.	Py	Ave.	Pmax	Ave.	δu	Ave.	μ	Ave.
Tensile Test	1	120.7	118.3	78.7	78.4	112.7	112.9	24.3	25.2	24.5	25.7
	2	119.1		77.7		111.1		26.1		26.6	
	3	115.0		78.8		115.0		25.3		26.0	
Compression Test	1	124.9	107.1	79.7	79.0	115.5	116.5	10.1	11.1	9.1	8.5
	2	89.3		78.2		117.5		12.1		7.9	

3 PRELIMINARY EXPERIMENTS OF COLUMN BASE JOINT

3.1 SPECIMENS

Table 3 shows the list of specimens, Fig 5 shows the specimen size and shapes, Fig 6 shows the details of the GIR rod, and Fig 7 shows the details of the column base bracket.
The parameter of the specimen was the tree species. The tree species used were glued laminated timber composed of heterogeneous grade, Sugi (JIS: E65-F225) and Larch (JIS: E105-F300).

https://doi.org/10.52202/080513-0374

For the GIR rod, high toughness coupler and fully threaded anchoring bolt (M20, JIS: SS400) were used. Three GIR rods were placed across the depth of the column at both ends, 50 mm from the edge.
The plate of column base bracket had a thickness of 30 mm. To prevent the GIR rods from bearing shear forces, 5th round steel bars with mill scale (φ20.2, JIS:SNR490B) were installed as the shear connector.
The GIR rods and column base bracket were fastened using standard bolts (M20, JIS: SS400).
The adhesive used for filling of GIR was an epoxy resin adhesive, and the curing period was 7 days.

Table 3 List of specimens

Specimens Name	No.	Tree Species	Cross-Sectional Dimensions (mm)	Height to the Point of Loading (mm)
IC-210×600	1	Sugi (E65-F225)	210×600	2000
	2			
	3			
IP-210×600	1	Larch (E105-F300)		

Specimens Name	No.	Number of GIR rod	Embedment Length of GIR rod (Anchorage Length) (mm)	Number of Shear Connector	Embedment Length of Shear Connector (mm)
IC-210×600	1	6	520 (380)	8	200
	2				
	3				
IP-210×600	1				

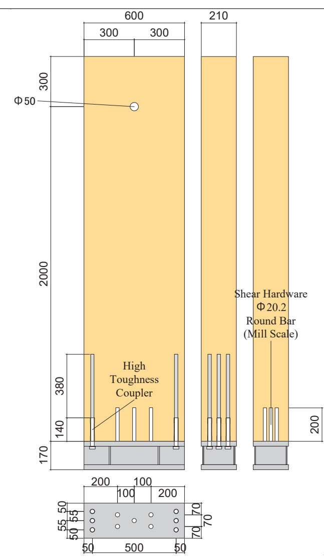

Fig.5 Specimen size and shapes

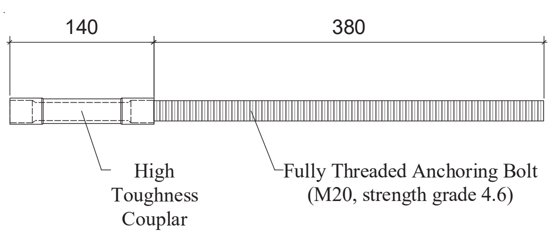

Fig.6 Details of the GIR rod

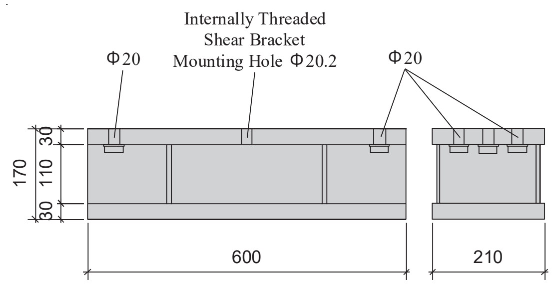

Fig.7 Details of the column base bracket

3.2 METHOD OF PRELIMINARY EXPERIMENTS OF COLUMN BASE JOINT

Fig 8 shows the loading apparatus, and Fig 9 shows the measurement method.
The drift angle of the column (R), and the rotation angle of the joint (θ) were measured. The loading schedule was controlled based on the observed R.
A static reversed cyclic loading test was performed, with three cycles ranging from 1/450 rad to 1/30 rad. Subsequently, monotonic loading was applied until failure or until reaching 1/15 rad.

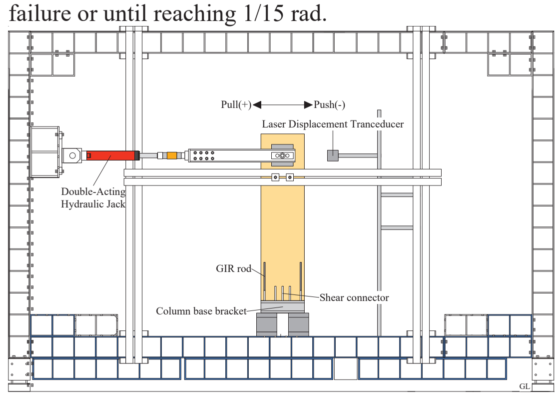

Fig.8 Loading apparatus

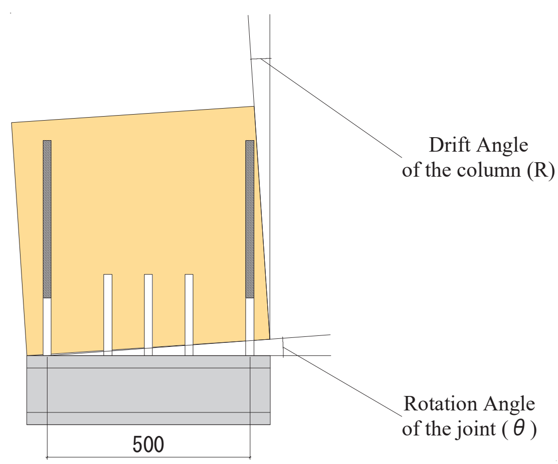

Fig.9 Measurement method

3.3 RESULTS AND DISCUSSIONS

Fig.10 shows the typical moment(M)-rotation angle of the joint(θ)relationship, Fig.11 shows the typical failure mode, and Fig.12 shows the shear connector before and after the test.
All specimens maintained high stiffness up to the 6th cycle (R=1/75 rad) and exhibited yielding behavior in the 7th cycle (R=1/50 rad). Thereafter, the load gradually increased while forming large hysteresis loops, and the test was terminated after pulling through the 9th cycle (R=1/15 rad). After the test, no fracture was observed in the high toughness coupler, but bending of the plate of column base bracket was confirmed.
For the shear connector, the mill scales on the steel bars before the test peeled off after the test. This suggests that the shear connectors resist not only the shear force but also the tensile force due to excessive adhesion.

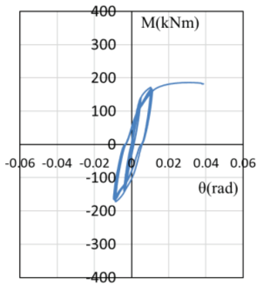

IC-210×600 No.1
Fig.10 M-θ relationship

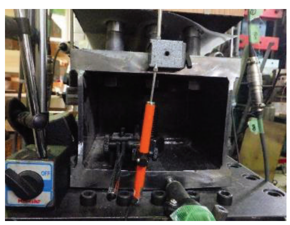

IC-210×600 No.1
Fig.11 Failure mode

Before the test After the test
Fig.12 Shear connecter

4 PULL-OUT TEST OF SHEAR CONNECTOR

4.1 SPECIMENS

Table 4 shows the list of specimens.
The shear connector was made from plain round bars (φ22,JIS: SNR490B) with externally threaded processing applied to one end. A total of eight surface treatment conditions were used: untreated (mill scale), polished, anti-rust spray, silicone spray, hot-dip galvanizing, phosphate treatment (a process that forms a lubricating film on the surface during press processing of automotive parts to reduce friction between the material and the mold), phosphate treatment after one month of exposure, and curing tape.
For the base material of the test specimens, glued laminated timber composed of heterogeneous grade, specifically Sugi (JIS: E65-F225) was used. The embedment length of the shear connector was set to 150 mm. Three specimens were prepared for each surface treatment condition, resulting in a total of 24 specimens.

Table 4 List of specimens

Surface Treatment	Tree Species	Cross-Sectional Dimensions (mm)	Shear Connector	Embedment Length Of Shear Connector (mm)
Untreated (mill scale)	Sugi (E65-F225)	1592×600	Plain Round Bars (φ22:SNR490B)	150
Hot-Dip Galvanizing				
Polished				
Anti-Rust Spray				
Silicone Spray				
Phosphate Treatment				
Phosphate Treatment After One Month Of Exposure				
Curing Tape				

4.2 METHOD OF PULL-OUT TEST OF SHEAR CONNECTOR

Fig.13 shows the test set-up for Pull-out test of shear connector.
A universal testing machine was used for loading, and monotonic tension and loading were applied at a speed of 1.0 mm/min.

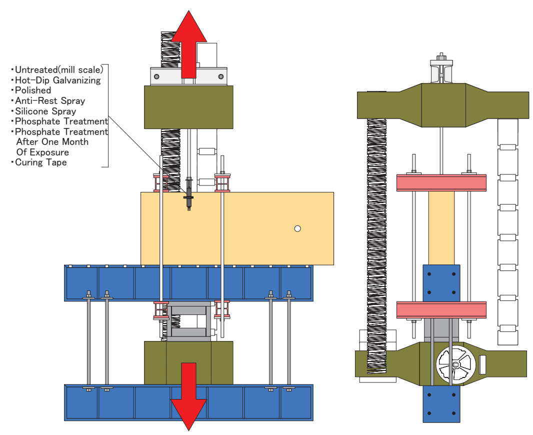

Fig.13 Loading apparatus

4.3 RESULTS AND DISCUSSIONS

Fig. 14 shows the maximum load for each series.
The maximum load was found to be lower in the specimens with the phosphate treatment and the use of curing tape.
Considering constructability, the surface treatment of the shear connector was chosen to be phosphate treatment in the following column base joint tests.

https://doi.org/10.52202/080513-0374

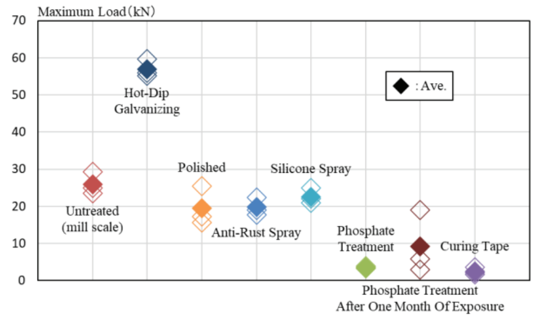

Fig.14　Maximum load

5 COLUMN BASE JOINT TEST

5.1 SPECIMENS

Table 5 shows the list of specimens, Fig 15 shows the specimen shapes, and Fig 16 shows the details of the column base bracket.

The parameters of the specimen are the tree species, cross-sectional dimensions, and the number of GIR rods. The tree species used were glued laminated timber composed of heterogeneous grade, Sugi (JIS: E65-F225) and Larch (JIS: E105-F300). The depths of the column were set to three types: 390 mm, 600 mm, and 800 mm, while the width of all specimens was 210 mm.

The details of GIR rods were the same as in the preliminary experiments. For IC-210×390-IMP1, 2 GIR rods were placed at 50 mm from both edges on the depth of the column. For IC-210×600-IMP1, IP-210×600-IMP1, and IC-210×800-IMP1, 3 GIR rods were placed across the depth of the column at both ends, 50 mm from the edge. For IC-210×800×2900-IMP1, 5 GIR rods were arranged in 2 tiers, 3 rods were placed at 50 mm from both edges on the depth of the column, and the other 2 rods were placed at 100 mm from both edges on the depth of the column.

The thickness of column base bracket plate was changed to 36 mm to withstand bending. To prevent the GIR rods from bearing shear forces, round steel bars (φ20.2,JIS: SNR490B) treated with the phosphate treatment were installed as the shear connector.

The GIR rods and column base bracket were fastened using the same method as in the preliminary experiments. The adhesive used for filling of GIR was an epoxy resin adhesive, and the curing period was 7 days.

Table 5　List of specimens

Specimens Name	No.	Tree Species	Cross-Sectional Dimensions (mm)	Height to the Point of Loading (mm)
IC-210×390-IMP1	1	Sugi (E65-F225)	210×390	2000
IC-210×600-IMP1	1		210×600	
	2			
	3			
IP-210×600-IMP1	1	Larch (E105-F300)		
IC-210×800-IMP1	1	Sugi (E65-F225)	210×800	
IC-210×800×2900-IMP1	1			2600

Specimens Name	No.	Number of GIR rod	Embedment Length of GIR rod (Anchorage Length) (mm)	Number of Shear Connector	Embedment Length of Shear Connector (mm)
IC-210×390-IMP1	1	4	520 (380)	4	200
IC-210×600-IMP1	1	6		8	
	2				
	3				
IP-210×600-IMP1	1				
IC-210×800-IMP1	1			11	
IC-210×800×2900-IMP1	1	10			

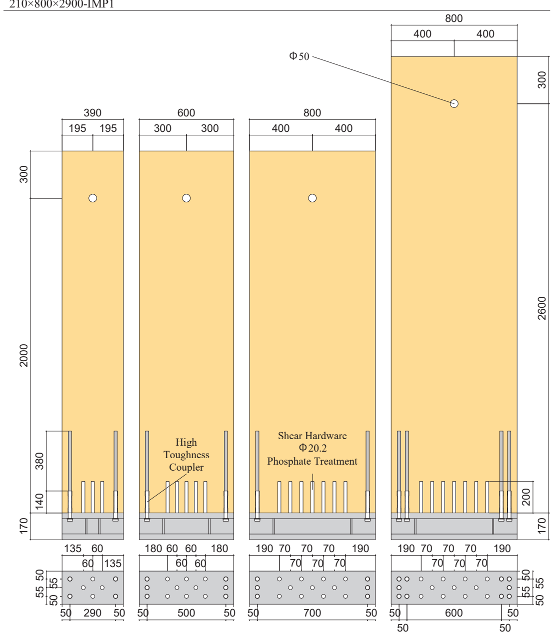

Fig.15　Specimen size and shapes

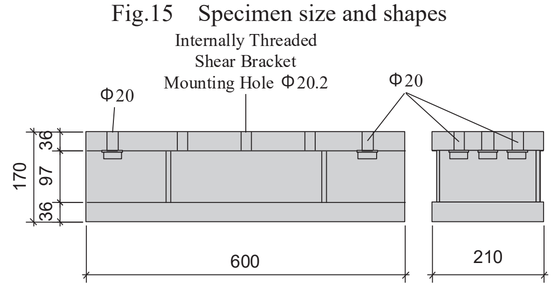

Fig.16　Details of the column base bracket

5.2 METHOD OF COLUMN BASE JOINT TEST

The test method was the same as that used in the preliminary experiments.

5.3 RESULTS AND DISCUSSIONS

5.3.1 M-θ RELATIONSHIP AND FAILURE MODE

Fig.17 shows the typical moment(M)-rotation angle of the joint(θ)relationships, while Fig.18 shows the typical failure modes.

IC-210×390-IMP1 maintained high stiffness up to the 7th cycle (R=1/50 rad) and exhibited yielding behavior in the 8th cycle (R=1/30 rad). Subsequently, a load drop occurred during the third pull of the 8th cycle. The failure mode was the bond failure of the GIR rod.

For IC-210×600-IMP1 and IP-210×600-IMP1, all specimens maintained high stiffness up to the 6th cycle (R=1/75 rad) and exhibited yielding behavior in the 7th cycle (R=1/50 rad). thereafter, the load gradually increased while forming large hysteresis loops, and the high toughness coupler fractured immediately after the completion of the 9th cycle (R=1/15 rad). The failure mode was fracture of the high toughness coupler in almost all specimens. However, in the case of IC-210×600-IMP1 No.1, the failure mode involved both fracture of the high toughness coupler and bond failure of the GIR rod.

IC-210×800-IMP1 maintained high stiffness up to the 6th cycle (R=1/75 rad), and exhibited yielding behavior in the 7th cycle (R=1/50 rad). Thereafter, during the 9th cycle (R=1/15 rad) at rotation angle of the joint corresponding to R=1/95 rad, splitting extended to the upper part of the specimen at the shear connector position.

In the M-θ relationship of IC-210×800×2900-IMP1, the distance from the loading point to the joint was relatively long, and the wood was highly deformed. Consequently, a discrepancy was observed between the drift angle of the column (R) and the rotation angle of the joint (θ). High stiffness was maintained up to the 7th cycle (R=1/50 rad), and yielding behavior was observed in the 8th cycle (R=1/30 rad). Thereafter, a load drop occurred during the second pull of the 8th cycle. The failure mode involved fracture of the high toughness coupler and bond failure of the GIR rod.

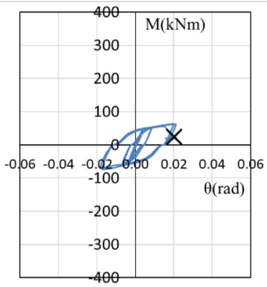

IC-210×390-IMP1

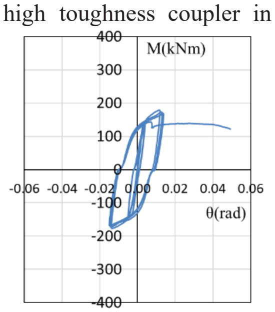

IC-210×600-IMP1 No.1

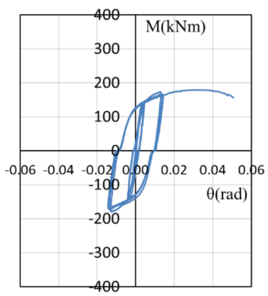

IC-210×600-IMP1 No.2

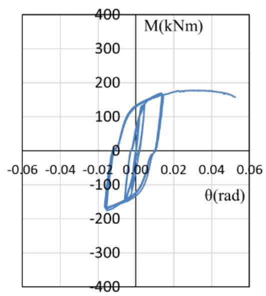

IP-210×600-IMP1

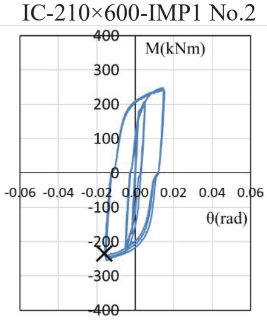

IC-210×800-IMP1

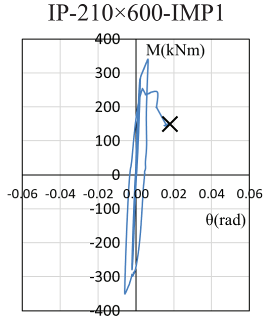

IC-210×800×2900-IMP1

Fig.17 Typical M-θ relationships

IC-210×390-IMP1
Bond failure of the
anchoring bolt

IC-210×600-IMP1 No.1
Fracture of the
high toughness coupler

IC-210×600-IMP1 No.2
Fracture of the
high toughness coupler

IC-210×600-IMP1 No.2
No bond failure of the
anchoring bolt

IP-210×600-IMP1
Fracture of the
high toughness coupler

IC-210×800-IMP1
Splitting extended to the
upper part of the specimen

IC-210×800×2900-IMP1
Fracture of the
high toughness coupler

IC-210×800×2900-IMP1
Bond failure of the
anchoring bolt

Fig.18 Typical failure modes

https://doi.org/10.52202/080513-0374

5.3.2 COMPARISON BETWEEN THE PRELIMINARY EXPERIMENTS AND COLUMN BASE JOINT

Fig.19 shows a comparison of the M-θ relationship between the preliminary experiments and column base joint test.

The specimens from the column base joint tests showed larger hysteresis loops than in the preliminary experiments. From this it can be concluded that the deformation performance has improved.

As regards failure modes, no failure of the high-toughness couplers was observed in the preliminary tests because the couplers were not sufficiently elongated by the bending of the column base bracket plates. On the other hand, in the column base joint tests, fracture of the high-toughness couplers was observed in almost all specimens, indicating that the behaviors of the couplers was in accordance with their design.

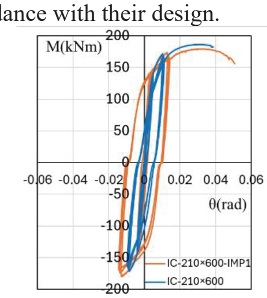

Fig.19 Comparison of the M-θ relationship between the preliminary experiments and column base joint test

5.3.3 COMPARISON OF CHARACTERISTIC PROPERTIES

Fig.20 to 23 show a comparison of the characteristic values for each specimen type. Furthermore, the rotational stiffness here is defined as the slope of the line connecting the points corresponding to 0.1 and 0.4 times the maximum load on the M-θ relationship.

5.3.3.1 COMPARISON BASED ON DEPTH OF COLUMN

The rotational stiffness of IC-210×800-IMP1 was 2.0 times higher than the average value of IC-210×600-IMP1. Furthermore, it was observed that both yield strength and ultimate strength increased almost in proportion to the increase in column depth.

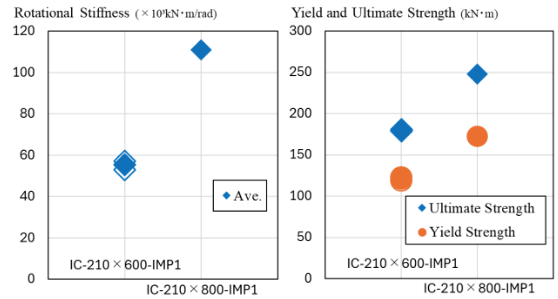

Fig.20 Comparison based on cross-section

5.3.3.2 COMPARISON BASED ON TREE SPECIES

A comparison of the rotational stiffness between IC-210×600-IMP1 and IP-210×600-IMP1 revealed that the value for Sugi was approximately 1.1 times higher than that for Larch. Furthermore, the yield strength and ultimate strength were found to be nearly equivalent. This result suggests that strength is primarily determined by the strength of the GIR rod and is not affected by the difference in tree species.

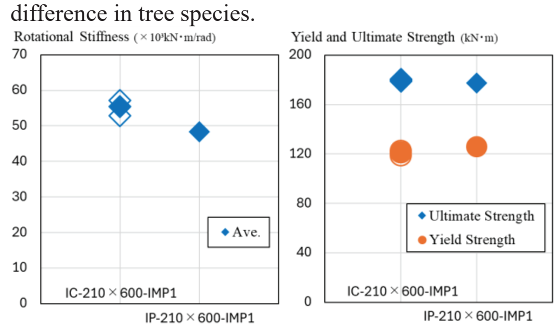

Fig.21 Comparison based on tree species

5.3.3.3 COMPARISON BASED ON THE NUMBER OF GIR RODS

A comparison between IC-210×800×2900-IMP1 and IC-210×800-IMP1 showed that the number of GIR rods increased by a factor of 1.6, while rotational stiffness increased by a factor of 1.5, and both yield strength and ultimate strength increased by a factor of 1.3. This difference is due to the different arrangements of GIR rods in IC-210×800-IMP1 and IC-210×800×2900-IMP1. IC-210×800-IMP1 has a single-layer arrangement (three wires) while IC-210×800×2900-IMP1 has a two-layer arrangement (three rods in the first layer and two rods in the second layer). As a result, the properties did not show a proportional relationship with the number of rods.

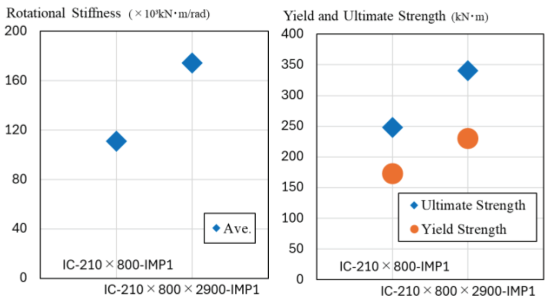

Fig.22 Comparison based on the number of GIR rods

5.3.3.4 STRUCTURAL CHARACTERISTIC COEFFICIENT

Fig.13 shows the structural characteristic coefficient of each test specimen. The Structural Characteristic Coefficient is a coefficient that evaluates the energy absorption capacity associated with plastic deformation capacity and damping characteristics.

Plasticity Ratio μ: It is the ratio of the displacement δu at yield to the displacement δv at ultimate failure.

$$\mu = \frac{\delta u}{\delta v}$$

Structural Characteristic Coefficient Ds: More ductile structures exhibit smaller values.

$$Ds = \frac{1}{\sqrt{2\mu - 1}}$$

For almost all specimens in the IC-210×600-IMP1, IP-210×600-IMP1, and IC-210×800-IMP1 series, the structural characteristic coefficient was 0.3 or lower, indicating high deformation capacity. On the other hand, for IC-210×390-IMP1, IC-210×600-IMP1 No.1, and IC-210×800×2900-IMP1, the bond failure of the GIR rods occurred before the coupler reached the target displacement. As a result, the ultimate deformation angle became smaller, leading to an increase in the structural characteristic coefficient.

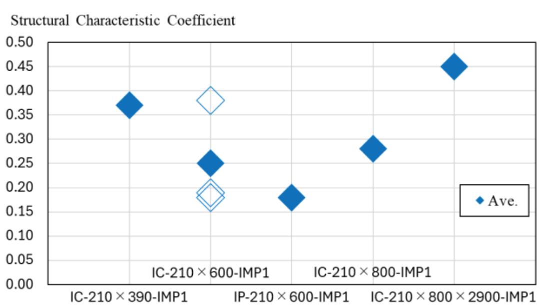

Fig.23 Structural characteristic coefficient

6 CONCLUSION

In this study, tensile and compression tests were conducted to evaluate the performance of high toughness couplers, as well as tensile tests of shear connectors and horizontal loading tests of GIR joints using high toughness couplers on column base joints.

In the tensile and compression tests of the coupler, it was confirmed that it possesses not only the target strength but also deformation capacity.

For the surface treatment of the shear connector in the column base joint tests, a phosphate treatment with relatively low maximum load was adopted based on the results of the shear connector tensile test.

In terms of the failure modes of the column base joint tests, specimens in which the fracture of the high toughness coupler occurred as expected exhibited a structural characteristic coefficient of 0.3 or lower, indicating high deformation capacity. However, in the specimens where bond failure of the GIR rods occurred, the coupler did not reach the target displacement, and due to the reduced ultimate displacement, the structural characteristic coefficient increased.

In the future, the balance between the wall thickness of the coupler and the length of the fixing section of GIR rod needs to be improved in order to solve the problems related to the adhesion breakage of GIR rod that occurred in some of the specimens.

7 REFERENCE

[1] J.Inoue, “Pull-Out and Moment Resisting Test of Glued-In Rod Joint Using Toughness Metal Connector” WCTE2018 CON-P-03

https://doi.org/10.52202/080513-0374